Research on surface photovoltage spectroscopy for GaAs photocathodes with $Al_xGa_{1-x}As$ buffer layer

Shuqin Zhang (张淑琴)[1,2], Liang Chen (陈 亮)[2*], and Songlin Zhuang (庄松林)[1]

[1]*Institute of Optical Electronic Information and Computer Engineering, University of Shanghai for Science and Technology, Shanghai 200093, China*

[2]*Institute of Optoelectronics Technology, China Jiliang University, Hangzhou 310018, China*

[*]*Corresponding author: 52571497@qq.com*

Received March 26, 2012; accepted May 17, 2012; posted online September 14, 2012

Surface photovoltage spectroscopy equations for cathode materials with an $Al_xGa_{1-x}As$ buffer layer are determined in order to effectively measure the body parameters for transmission-mode (t-mode) photocathode materials before Cs-O activation. Body parameters of cathode materials are well fitted through experiments and fitting calculations for the designed $Al_xGa_{1-x}As$/GaAs structure material. This investigation examines photo-excited performance and measurements of body parameters for t-mode cathode materials of different doping structures. It also helps study various doping structures and optimize structure designs in the future.

OCIS codes: 040.7190, 160.1890, 230.0040, 260.7210.

doi: 10.3788/COL201210.110401.

After Cs-O activation, the surface barriers of GaAs photocathodes can become negative electron affinity (NEA), driving photo-excited electrons to tunnel through surface barriers into a vacuum. Thus, NEA GaAs photocathodes have been widely used in night-vision image intensifiers, photomultiplier tubes, and polarized electron sources due to their excellent wavelength response, high quantum efficiency, and good spin polarization[1]. NEA photocathodes are of two types: a reflection-mode (r-mode) cathode, in which the incident light and electron emission surface are on the same side, and a transmission-mode (t-mode) cathode, in which the incident light and electron emission surface are on different sides. In practical applications, NEA photocathodes often operate in t-mode, but the measurement techniques for t-mode cathode materials before activation are inadequate[2].

As the buffer layer matching the lattice between the Si_3N_4 antireflective film and GaAs active layer, the $Al_xGa_{1-x}As$ layer helps reflect the photo-excited electrons to the active layer and finally promotes quantum efficiency for NEA photocathodes. In previous studies, the measurements for GaAs photocathodes mainly depend on the spectral response curve (SRC) after activation. However, the parameters of GaAs photocathodes cannot be effectively measured by SRC alone, because the performances of cathodes after activation are influenced not only by material parameters mainly connected with the doping structure and epitaxial growth technique, but also by surface barriers mainly related to Cs-O activation techniques. Surface photovoltage spectroscopy (SPS) is connected only to the performance of cathode materials. Thus, in recent research, SPS has been widely used to measure material parameters, such as electron diffusion length and interface recombination velocity, for cathode materials with an r-mode structure. A comparative research between SPS before activation and SRC after activation has also exactly fitted the surface escape probability[3]. The SPS fitting theory is inadequate for the t-mode material, which has a more complex structure than the r-mode cathode. Thus, the SPS research for cathode materials with the $Al_xGa_{1-x}As$ buffer layer can help in further building the SPS theory for t-mode photocathodes[4].

The main difference between the t-mode and r-mode structures is the $Al_xGa_{1-x}As$ buffer layer. Figure 1 shows the complete t-mode cathode module in the glass/Si_3N_4/$Al_xGa_{1-x}As$/GaAs/pole structure. Thus, we focused on the $Al_xGa_{1-x}As$/GaAs structure material, which simplified the SPS research by removing other layers of the t-mode cathode module. The cathode material was designed by molecular beam epitaxial (MBE) with p-type beryllium Be doping. Figure 2 shows the material structure, where the GaAs substrate has been grown with high-quality p-type doping concentration of about 1.0×10^{18} cm^{-3}. The $Al_xGa_{1-x}As$ buffer layer was designed with a Be doping concentration of 2.0×10^{18} cm^{-3} and Al mole fraction of 0.63.

The Al mole fraction is 0.63, because the lattice constant of $Al_xGa_{1-x}As$ material is calculated by[5]

$$a_{Al_xGa_{1-x}As} = 5.6533 + 0.078x. \quad (1)$$

When the Al mole fraction x=0.63, the lattice constant of the $Al_xGa_{1-x}As$ material is 5.7024×10^{-10} m in accordance with that of GaAs material at 5.6533×10^{-10} m. First, the cathode material was allowed to pass successively through acetone, hydrofluoric acid, and absolute

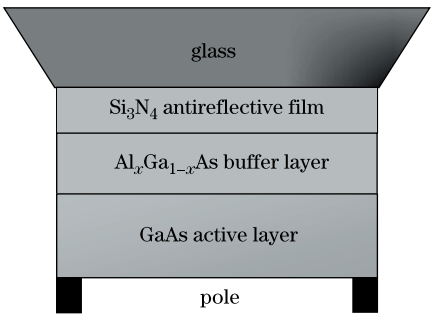

Fig. 1. Diagram of the t-mode photocathode module.

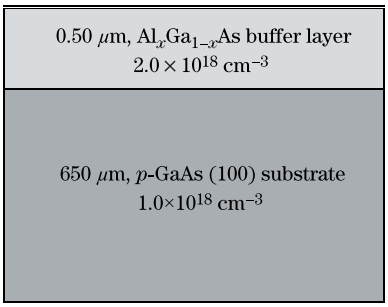

Fig. 2. Diagram of the photocathode material with the $Al_xGa_{1-x}As$ buffer layer.

ethyl alcohol by ultrasonic washing for about 5 min. This was done to remove surface oxidation and impurities. Then the cathode material was placed into the SPS measurement system, as illustrated by the schematic block diagram in Fig. 3. When the measurement began, white light was allowed to pass through the grating monochromator and light chopper. This was then modulated into monochromatic light and irradiated through optical fiber on the cathode material. The cathode material was placed between two indium tin oxide (ITO) glasses and into a steel pool with constant temperature to shield off sound, electromagnetism, and other interferences[6]. The SPS signal was finally amplified by a lock-in amplifier system and then sent to the computer through a serial port. The power light irradiating on the cathode material was maintained at about 200 nW, and the light chopper frequency was controlled to 30 Hz. Anhydrous ethanol was placed between the front ITO glass and cathode material to form the metal/insulator/semiconductor (MIS) interaction structure, thus gaining better signal-to-noise ratio (SNR). When the periodic light irradiates the MIS structure, the photo-excited electrons would not reach the bottom ITO glass, and the surface photovoltage between two ITO glasses would depend on the variation of interaction electrons at the top ITO glass.

Previous fitting equations for the GaAs active layer/GaAs substrate r-mode cathode materials cannot be adapted for this $Al_xGa_{1-x}As$/GaAs/GaAs structure. Hence, a new fitting equation must be determined. The electron potential barrier between the GaAs active layer and the $Al_xGa_{1-x}As$ buffer layer are calculated by[7]

$$\Delta E_c = \Delta E_g - \Delta E_V, \tag{2}$$

$$\Delta E_V = (E_F - E_{V1}) - (E_F - E_{V2}), \tag{3}$$

where E_F is the unity Femi level for $Al_xGa_{1-x}As$ and GaAs by the Femi-level effect; E_g is the bandwidth; E_{V1} and E_{V2} are the valence band maxims of $Al_xGa_{1-x}As$ and GaAs, respectively. Thus, the band bending structure of the GaAs/$Al_xGa_{1-x}As$ hetero-junction is determined by the discontinuities in the conduction bands ΔE_c. For the GaAs material, the bandwidth E_{g2} is about 1.424 eV at room temperature, whereas for $Al_xGa_{1-x}As$, the bandwidth E_{g1} depends on the Al content x[8], and is given by

$$E_{g1} = \begin{cases} 1.424 + 1.247x, (0 \leqslant x \leqslant 0.45) \\ 1.424 + 1.247x + 1.147(x-0.45)^2, \ (0.45 \leqslant x \leqslant 1.0) \end{cases}. \tag{4}$$

The Al mole fraction is $x = 0.63$, and thus, the value of E_{g1} is calculated as 2.247 eV. Furthermore, the values of $E_F - E_{V1}$ and $E_F - E_{V2}$ are calculated using the carrier concentration P measured by the Bio-Rad electrochemical voltage (ECV) profiling as[9]

$$E_F - E_V = k_0 T \ln(N_V/P), \tag{5}$$

$$N_V = 2.5 \times 10^{19} (m_p/m_0)^{3/2} (T/300)^{3/2}, \tag{6}$$

where N_V is the effective density of states for the valence bands of the p-type GaAs/ $Al_xGa_{1-x}As$ epilayers. For the GaAs material, m_p/m_0=0.48, whereas for the $Al_xGa_{1-x}As$ material, m_p/m_0 depends on the Al mole fraction calculated by

$$m_p = (0.48 + 0.31x) m_0. \tag{7}$$

Thus, the final calculation for the band bending between GaAs/$Al_xGa_{1-x}As$ epilayers can be deduced as

$$\Delta E_c = 1.247x + 1.147(x-0.45)^2 - (300k_0/1.6\times10^{-19}) \times \ln\{(P_2/P_1)[1 + (0.31x/0.48)^{3/2}]\}. \tag{8}$$

Through the ECV curve for the designed material, the band bending energy between GaAs/$Al_xGa_{1-x}As$ epilayers are calculated as 0.785 eV. This band bending region between the GaAs/$Al_xGa_{1-x}As$ interfaces forms an internal space charge region for the designed material[9].

Therefore, in case of the difference of electron work functions between the ITO glass and the $Al_xGa_{1-x}As$ buffer layer, two space charge regions for the designed material are the ITO/$Al_xGa_{1-x}As$ and the $Al_xGa_{1-x}As$/GaAs interfaces as per SPS measurement. The entire material SPS working mechanism appears as two capacitances of series connection, which is shown as Fig. 4[10].

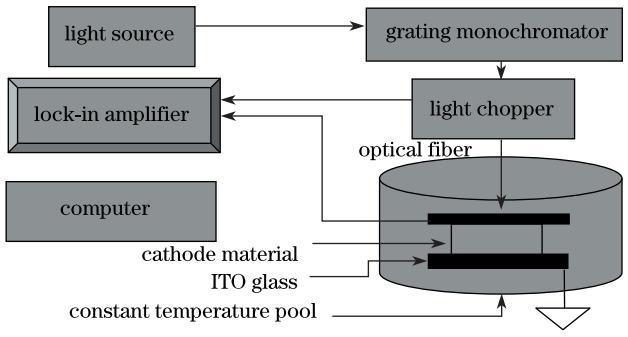

Fig. 3. Diagram of the SPS measurement system.

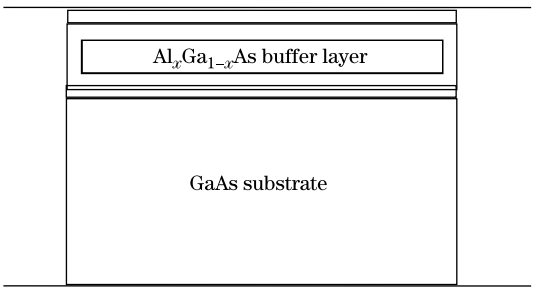

Fig. 4. SPS working mechanism for the designed material.

The GaAs substrate is about 650 μm in depth. Thus, the photo-excited electrons cannot reach the bottom of the GaAs substrate, and the bottom ITO glass only seems to be the contact electrode. Furthermore, the widths of the space charge regions are much smaller than those of the doping layers. When the SPS signal becomes stable, there must be one dynamic equilibrium place near the front ITO glass/$Al_xGa_{1-x}As$ buffer layer interface, where the body diffusion current from the doping layer equals the electric drift current from the space electron region. At this boundary space, the recombination velocity of photo-excited electrons appears very large. Thus, using the ITO/$Al_xGa_{1-x}As$ interface as the starting coordinate, the boundary conditions of the $Al_xGa_{1-x}As$ buffer layer is given as[10]

$$D_{\rm n}\frac{{\rm d}\Delta n(x)}{{\rm d}x}\Big|_{x=T_{\rm e1}} = S_{\rm v}\Delta n(x), \quad \Delta n(x)\Big|_{x=0} = 0, \quad (9)$$

where $D_{\rm n}$ is the electron diffusion coefficient, $T_{\rm e1}$ is the depth of $Al_xGa_{1-x}As$ buffer layer, and $S_{\rm v}$ is the recombination velocity at the $Al_xGa_{1-x}As$/ GaAs interface. For the GaAs doping substrate, using the bottom of the space charge region at the $Al_xGa_{1-x}As$/GaAs interface, the boundary conditions can be set as

$$D_{\rm n}\frac{{\rm d}\Delta n(x)}{{\rm d}x}\Big|_{x=0} = S_{\rm v}\Delta n(x), \quad \Delta n(\infty) = 0. \quad (10)$$

Meanwhile, the one-dimensional diffusion equation for the no equilibrium minority carriers of GaAs cathode materials[9] is given by

$$D_{\rm n}\frac{{\rm d}^2\Delta n(x)}{{\rm d}x^2} - \frac{\Delta n(x)}{\tau} + \alpha I_0(1-R)\exp(-\alpha x) = 0, \quad (11)$$

where τ is the electron lifetime, $T_{\rm e}$ is the doping layer thickness, R is the material reflectivity, α is absorption coefficient, and I_0 is the incident light intensity[11].

In accordance with the photodiode theory, the theoretical SPS equations are shown as

$$V = \frac{KT}{q}\ln\left(1+\frac{J_{\rm w}}{J_0}\right), \quad J_{\rm w} = D_{\rm n}\frac{{\rm d}n(x)}{{\rm d}x}\Big|_{x=0}, \quad (12)$$

where V is the SPS value for the cathode material, $J_{\rm w}$ is the photo-excited current flowing to the space charge region from the doping layer, and J_0 is the saturated current for the cathode material. Using the deductions made in Eqs. (9)–(12), the SPS equations for the $Al_xGa_{1-x}As$/GaAs cathode materials are shown as

$$\begin{cases} V_1 = \dfrac{KT}{q}\ln\left(1+\dfrac{J_{Al_xGa_{1-x}As}}{J_{01}}\right) \\ V_2 = \dfrac{KT}{q}\ln\left(1+\dfrac{J_{\rm GaAs}}{J_{02}}\right), \quad V = V_1 + V_2 \end{cases}, \quad (13)$$

where J_{01} and J_{02} are the saturated currents for the two layers, respectively, $J_{Al_xGa_{1-x}As}$ and $J_{\rm GaAs}$ are photo-excited current for two layers, which are shown as

$$J_{Al_xGa_{1-x}As} = \frac{qI_0(1-R)\alpha_1 L_1}{\alpha_1^2 L_1^2 - 1} \times \left[\frac{(S_{\rm v}-\alpha_1 D_{\rm n})\exp(-\alpha_1 T_{\rm e1})}{(D_{\rm n}/L_1)\cosh(T_{\rm e1}/L_1) + S_{\rm v}\sinh(T_{\rm e1}/L_1)} - \frac{S_{\rm v}\cosh(T_{\rm e1}/L_1) + (D_{\rm n}/L_1)\sinh(T_{\rm e1}/L_1)}{(D_{\rm n}/L_1)\cosh(T_{\rm e1}/L_1) + S_{\rm v}\sinh(T_{\rm e1}/L_1)} + \alpha_1 L_1\right], \quad (14)$$

$$J_{\rm GaAs} = qI_0(1-R)\exp(-\alpha_1 T_{\rm e1})\frac{\alpha_2 L_2}{1+\alpha_2 L_2}\frac{L_2 S_{\rm v}}{D_{\rm n}+S_{\rm v}L_2}, \quad (15)$$

where α_1 and α_2 are the material absorption coefficients for the $Al_xGa_{1-x}As$ and GaAs doping layers, respectively; L_1 and L_2 are the electron diffusion lengths for each layer[12].

Thus, through the fitting calculations for experimental normalized SPS curve by equal photon number, the body parameters of the designed cathode material can be fitted well. Although the saturation current cannot be exactly measured, Eq. (13) shows that the exact saturation value does not influence the shape of the SPS curve, and the final influence is the ratio of J_{01}/J_{02} for the two doping layers.

For fitting calculations, Fig. 5 shows the absorption coefficient α_1 of the GaAs doping substrate.

Figure 6 shows the absorption coefficient α_2 of $Al_xGa_{1-x}As$ doping buffer layer.

Figure 7 shows the experimental and fitting curves of the SPS for the designed cathode material. For the fitting calculation, the value of $D_{\rm n}$ is set as $1.1\times10^{10}\mu m^2/s$,

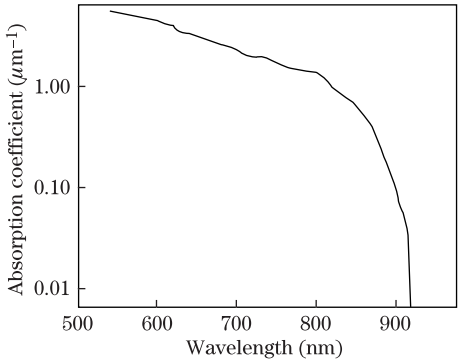

Fig. 5. Absorption coefficient for the GaAs doping layer at 300 K.

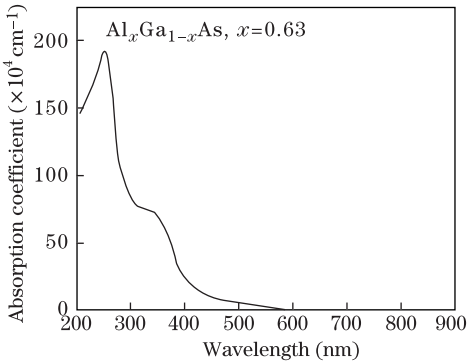

Fig. 6. Absorption coefficient of the $Al_xGa_{1-x}As$ buffer layer.

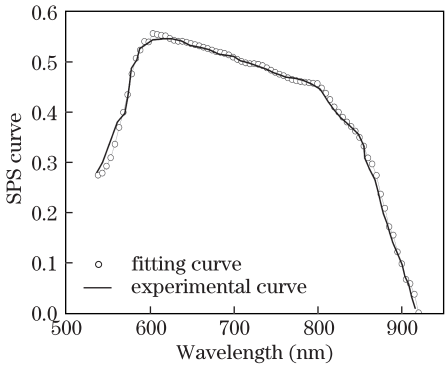

Fig. 7. Experimental and fitting SPS curves for the designed material.

and the fitting parameters for the cathode material are L_1=0.5 μm and L_2=3.1 μm; the ratio of saturation current for the two doping layers is J_{01}/J_{02}=4; the recombination velocity of $Al_xGa_{1-x}As$/GaAs interface is S_v=1.0×10^{10} μm/s.

Through fitting calculations, the major parameters of the designed material, such as the electron diffusion length and interface recombination velocity, are effectively measured. From this, we can determine the body parameters and evaluate the photo-excited performance for photocathode materials with the $Al_xGa_{1-x}As$ buffer layer in future research.

In conclusion, the SPS equations for cathode materials with the $Al_xGa_{1-x}As$ buffer layer are determined based on early SPS research for r-mode photocathode materials. This is conducted to measure the parameters for t-mode photocathode materials before Cs-O activation. Through experiments and fitting calculations, the simple fitting equations effectively measure the major body parameters for the $Al_xGa_{1-x}As$/GaAs cathode materials. This research helps in gaining further understanding of SPS performance for t-mode photocathode materials. The results can also help optimize the varied doping structure designs for t-mode GaAs photocathodes in the future.

This work was supported by the General Administration for Quality Supervision of China (No. 2008QK328) and the Zhejiang Provincial Natural Science Foundation of China (No. Y5090150).

References

1. G. Faraci, A. R. Pennisi, F. Gozzo, S. La Rosa, and G. Margaritondo, Phys. Rev. B **53,** 3987 (1996).
2. J. J. Zou, B. K. Chang, Y. J. Zhang, and Z. Yang, Appl. Opt. **49,** 2561 (2010).
3. L. Chen, Y. S. Qian, and B. K. Chang, Appl. Opt. **50,** 7035 (2011).
4. W. Wang, Y. Huang, X. Duan, Q. Yan, X. Ren, S. Cai, J. Guo, and H. Huang, Chin. Opt. Lett. **9,** 111301 (2011).
5. Z. Yang, B. K. Chang, J. J. Zou, J. J. Qiao, P. Gao, Y. P. Zeng, and H. Li, Appl. Opt. **46,** 7035 (2007).
6. L. Chen, Y. S. Qian, Y. J. Zhang, and B. K. Chang, Opt. Commun. **284,** 4520 (2011).
7. J. Zhao, B. K. Chang, Y. J. Xiong, and Y. J. Zhang, Chin. Phys. B **20,** 47801 (2011).
8. Y. J. Zhang, J. Niu, J. Zhao, J. J. Zou, B. K. Chang, F. Shi, and H. C. Cheng, J. Appl. Phys. **108,** 093108 (2010).
9. J. Tousek and D. Kindl, J. Appl. Phys. **89,** 460 (2001).
10. Y. T. Cheng, Physica E **14,** 313 (2002).
11. M. A. Reshchikov, M. Foussekis, and A. A. Baski, J. Appl. Phys. **107,** 113535 (2010).
12. Y. Zhi, J. J. Zou, and B. K. Chang, Acta. Phys. Sin. **59,** 4290 (2010).